HHS Public Access

Author manuscript

Curr Biol. Author manuscript; available in PMC 2017 September 12.

Published in final edited form as:

Curr Biol. 2016 September 12; 26(17): 2379–2387. doi:10.1016/j.cub.2016.07.008.

Muscle- and skin-derived cues jointly orchestrate patterning of somatosensory dendrites

Carlos A. Díaz-Balzac[1], **Maisha Rahman**[2], **María I. Lázaro-Peña**[1], **Lourdes A. Martin Hernandez**[1], **Yehuda Salzberg**[1,§], **Cristina Aguirre-Chen**[2,¶], **Zaven Kaprielian**[2,†], and **Hannes E. Bülow**[1,2]

[1]Department of Genetics, Albert Einstein College of Medicine, Bronx, New York, 10461, USA

[2]Dominick P. Purpura Department of Neuroscience, Albert Einstein College of Medicine, Bronx, New York, 10461, USA

Summary

Sensory dendrite arbors are patterned through cell-autonomously and non-autonomously functioning factors [1–3]. Yet, only a few non-autonomously acting proteins have been identified, including semaphorins [4, 5], brain derived neurotrophic factors (BDNF) [6], UNC-6/Netrin [7], and the conserved MNR-1/Menorin–SAX-7/L1CAM cell adhesion complex [8, 9]. This complex acts from the skin to pattern the stereotypic dendritic arbors of PVD and FLP somatosensory neurons in *Caenorhabditis elegans* through the dendritic leucine rich transmembrane receptor DMA-1/LRR-TM on PVD neurons [8, 9]. Here we describe a role for the diffusible *C. elegans* protein LECT-2, which is homologous to vertebrate leukocyte cell-derived chemotaxin 2 (LECT2)/chondromodulin II. LECT2/chondromodulin II has been implicated in a variety of pathological conditions [10–13], but the developmental functions of LECT2 have remained elusive. We find that LECT-2/Chondromodulin II is required for development of PVD and FLP dendritic arbors, and can act as a diffusible cue from a distance to shape dendritic arbors. Expressed in body wall muscles, LECT-2 decorates neuronal processes as well as hypodermal cells in a pattern similar to the cell adhesion molecule SAX-7/L1CAM. LECT-2 functions genetically downstream of the MNR-1/Menorin–SAX-7/L1CAM adhesion complex, and upstream of the DMA-1 receptor. LECT-2 localization is dependent on SAX-7/L1CAM, but not on MNR-1/Menorin or DMA-1/LRR-TM, suggesting that LECT-2 functions as part of the skin-derived MNR-1/Menorin–SAX-7/L1CAM adhesion complex. Collectively, our findings suggest that muscle-derived LECT-2/

*corresponding author: Telephone 718 430 3621, Fax 718 430 8778, hannes.buelow@einstein.yu.edu.
§present address: Weizmann Institute, Rehovot, 7610001, Israel
¶present address: Cold Spring Harbor Laboratory, Cold Spring Harbor, NY 11724, USA
†present address: AMGEN, Cambridge, MA 02141, USA

Author contributions:

C.A.D.B, M.R. and H.E.B. conceived, and C.A.D.B, M.R., M.I.L.P, and L.A.M.H. performed experiments. Y.S., C.A.C., and Z.K. were involved during inception of the project, as well as isolation and initial characterization of the spontaneous *rz2* mutant allele. C.A.D.B, M.R., and H.E.B. analyzed the data and prepared the manuscript with editorial input from all authors.

Accession number

The sequence of the *lect-2* transcript has been submitted to GenBank under accession number KX255656.

Chondromodulin II acts as a muscle-derived, diffusible cofactor together with a skin-derived cell adhesion complex to orchestrate the molecular interactions of three tissues during patterning of somatosensory dendrites.

eTOC

Díaz-Balzac *et al.* show that muscle-derived LECT-2/Chondromodulin II serves as a diffusible cue to pattern sensory dendrite arbors in *Caenorhabditis elegans* together with a conserved skin-derived adhesion complex.

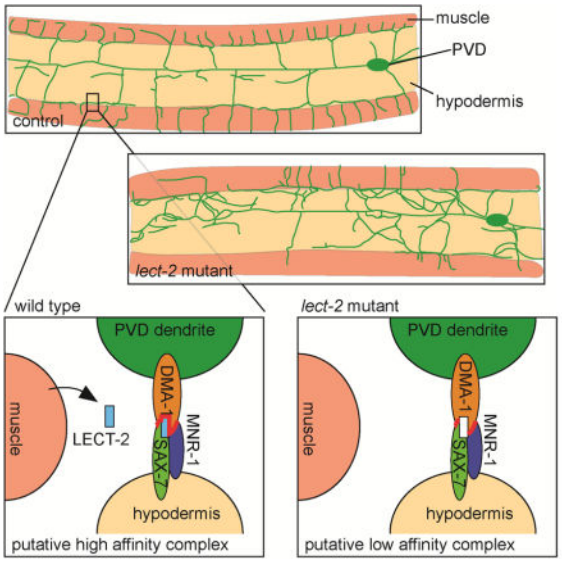

Results and Discussion

A LECT-2/Lect2 like protein is required for patterning of somatosensory dendrite arbors

PVD somatosensory dendrites are stereotypically patterned, through consecutive orthogonal branching of secondary, tertiary and quaternary branches from primary dendrites that emanate from the PVD cell bodies laterally towards the anterior and posterior of the animal, respectively (Fig. 1A)[14, 15]. Using forward genetic screens to identify genes involved in patterning of the stereotypic dendritic arborization of PVD neurons, we isolated mutant alleles of the *C. elegans* homolog of vertebrate Lect2/Chondromodulin II (Fig. 1, Fig. S1, Fig. S2, Supplemental Experimental Procedures). Altogether, we obtained thirteen mutant alleles including two deletions, a complex rearrangement, and two splice acceptor mutations (Fig. 1C, see Supplemental Experimental Procedures for details). Lect2/Chondromodulin II, originally identified as a growth promoting factor from bovine fetal cartilage [16], and a chemotactic factor from a leukemic cell line [17], is characterized by a conserved M23 peptidase domain. This domain is commonly found in prokaryotic genomes as part of zinc-dependent glycine-glycine lyases that degrade bacterial cell walls [18], but has also been shown to act as a protein-protein interaction domain [19, 20]. Lect2/Chondromodulin II is the only gene encoding the M23 domain found in mammals and nematodes. Four missense alleles (out of eight) changed conserved residues in the M23 peptidase domain and resulted

in defects in PVD patterning, suggesting that the M23 domain is important for function (Fig. 1C, Fig. S2).

To understand the developmental role of LECT-2, we conducted a detailed morphometric analysis of the dendritic arbor in PVD neurons of *lect-2(rz2)* mutant animals, which based on phenotype and molecular nature, is likely a complete loss-of-function allele (Supplemental Experimental Procedures). We measured the number and length of secondary, tertiary, quaternary, as well as ectopic tertiary dendrites in a section that extended 100μm anteriorly from the PVD cell body. Ectopic tertiary branches are branches that originate from secondary branches, but are not at the correct position along the boundary between muscle and hypodermis (Fig. 1A). We found that the number of secondary and ectopic tertiary branches was increased in *lect-2(rz2)* mutant animals (Fig. 1B), whereas the number of tertiary branches was reduced, as was the number of quaternary branches (Fig. 1B). Consistent with these changes in branch numbers, we found that the aggregate length of tertiary and quaternary branches was significantly reduced and the length of secondary and ectopic tertiary branches increased, albeit with less statistical certainty ($p=0.34$ and $p=0.03$, respectively, Fig. S3A). The observed abnormalities in dendrite patterning are already seen during larval stages suggesting that the *lect-2* mutant phenotype is a developmental rather than a maintenance defect (Fig. S3B). We conclude that the normal function of *lect-2* during development is to restrict secondary and ectopic tertiary dendritic branches and to promote the formation of stable higher order branches by either inhibiting their formation, or facilitating their pruning. Lastly, we observed defects in self-avoidance of dendritic branches in *lect-2* mutants (Fig. 1E), indicating that LECT-2 also functions in mediating self-avoidance between tertiary branches.

We next asked whether the patterning defects in *lect-2* mutants were specific to PVD dendrites or were also displayed by other neurons. We found no obvious defects in a number of sensory neurons, motor neurons, and interneurons, including ones that project neuronal processes along the ventral nerve cord (Table S1). We also established that *lect-2* was not required for general neurite branching, because we saw no effects on neuronal branching due to overexpression of the cell adhesion molecule KAL-1/Anosmin-1 [21](Table S1). However, we did observe disorganized FLP neurons with defects similar to those seen in PVD neurons (Fig. 1F). FLP neurons are a pair of neurons that form a similarly elaborate PVD-like dendritic tree and serve related functions, but cover the head and neck region of the animals, rather than the body [14, 15]. Since FLP and PVD (together with IL2 neurons in dauer animals [22]), comprise the most elaborate dendritic arbors in *C. elegans*, these finding suggest that *lect-2* is primarily required for dendritic branching rather than serving more general neuronal patterning functions.

LECT-2/Chondromodulin II is expressed in muscle and localizes to neural processes and hypodermal tissues

To determine where the *lect-2* gene is expressed, we first constructed a transcriptional reporter in which 3.4kb of 5′UTR upstream of the *lect-2* ATG (up to the 3′ end of the preceding gene) drives expression of mCherry (Fig. 2A). We found strong expression of this reporter in body wall muscle cells throughout life (Fig. 2A, data not shown). To determine

the subcellular localization of LECT-2, we conducted two sets of experiments: we first fused red fluorescent mCherry to the C-terminus of the *lect-2* cDNA and expressed this fusion under control of a muscle-specific (*Pmyo-3*) promoter. This protein fusion fully rescued the mutant phenotype and was localized to large parts of the nervous system (Fig. 2B). Interestingly, we also detected LECT-2::mCherry along the boundary of the lateral hypodermis and the muscle (Fig. 2B), where the tertiary dendritic branches of PVD are localized by a protein complex consisting of the MNR-1/Menorin and SAX-7/L1CAM cell adhesion molecules [8, 9]. To precisely determine the level and localization of endogenous LECT-2, we engineered the endogenous *lect-2* locus by CRISPR/Cas9 mediated gene editing [23] to express a C-terminal fusion of LECT-2 with mNeonGreen (Fig. 2C–E). We found that this translational fusion expressed diffusely from at least the gastrula stage to the threefold embryonic stage, at which time the fusion became more localized, possibly to cell-cell junctions (Fig. 2C). During larval and adult stages, LECT-2::mNeonGreen localized to basement membranes of hypodermal tissues, and processes of the nervous system, including commissures, sensory dendrites in the head, and lateral nerve tracts (Fig. 2C–E). In contrast, staining of neuronal cell bodies was less uniform. For example, neurons near the nerve ring in the head showed little or no staining (Fig. 2D), whereas cell bodies of motor neurons and some mechanosensory neurons cell bodies (e.g. ALM) showed staining (Fig. 2D, see also Fig. 4G). We also observed that LECT-2::mNeonGreen localized to the cell surface of a set of hypodermal cells named the seam cells, and along the boundary of the lateral hypodermis. Lastly, LECT-2::mNeonGreen is seen on the basement membranes of body wall muscles and along fibrous organelles (Fig. 2E, inset), the desmosome-like complexes that form the physical link between body wall muscle and hypodermis, and are juxtaposed with quaternary PVD branches [24]. Intriguingly, LECT-2::mNeonGreen localization was indistinguishable from the localization of a SAX-7/L1CAM::GFP reporter (Fig. 2E, F), including the colocalization of tertiary dendrites with the lateral hypodermal staining (cf. Fig. 2B and Fig. 2F).

LECT-2/Lect2 functions as a diffusible cue from muscle

To determine where LECT-2 functions, we conducted cell-specific rescue experiments and expressed a LECT-2 cDNA under the control of heterologous promoters, including from muscle (*Pmyo-3*), all neurons (*Prab-3*), the hypodermis (skin, *Pdpy-7*), the coelomocytes (*Punc-122*), the pharynx (*Pceh-22*), and the single pair of AIY interneurons (*Pttx-3*), which are located in the ventral ganglion in the head. We found that expression from all tissues, including to some extent from the quite distant pharynx and the single pair of AIY interneurons, rescued the mutant defects in PVD dendritic branching of *lect-2* mutant animals (Fig. 3). Moreover, we found the C-terminal fusions of LECT-2 with both mCherry and mNeonGreen in vesicles of the coelomocytes (Fig. 2B, 2D), which are known to uptake diffusible cues from the pseudocoelom [25]. Both the rescue experiments from anatomically distant tissues as well as the presence of the rescuing fusion proteins in coelomocytes suggest that LECT-2/Chondromodulin II can act as a secreted and diffusible cue. To determine whether LECT-2 must diffuse to function, we fused a heterologous transmembrane domain to the C-terminus of LECT-2, followed by a fluorescent protein to control for expression. This fusion expressed under a muscle specific (or pan-neuronal, hypodermal, or PVD-specific) promoter failed to rescue the *lect-2* mutant phenotype (Fig.

3C, D). Taken together, these experiments suggest that LECT-2 acts as a diffusible cue from body wall muscles to non-autonomously pattern the dendritic arbors of PVD somatosensory neurons.

LECT-2/Lect2 acts within the menorin pathway

The phenotypes we observed in *lect-2* mutant animals are similar to those of mutants in genes encoding the adhesion molecules MNR-1/Menorin, SAX-7/L1CAM or the DMA-1/LRR-TM receptor [8, 9]. We found that double mutants between *lect-2* and either *mnr-1/menorin* or *sax-7/L1CAM* were not more severe than either of the single mutants with respect to the total number and aggregate length of higher order and ectopic branches, suggesting that *lect-2* acts genetically in a pathway with both *mnr-1/Menorin* and *sax-7/L1CAM* (Fig. 4A–D, Fig. S3C). Moreover, double mutants between *lect-2* and the leucine rich transmembrane receptor *dma-1/LRR-TM* were indistinguishable from the *dma-1* single mutants with respect to secondary, tertiary, and quaternary branches, showing that *dma-1/LRR-TM*, which functions in PVD neurons [26], is epistatic to *lect-2*, and thus likely acts downstream of *lect-2*. To investigate the genetic relationship between *mnr-1/Menorin* and *lect-2*, we exploited a previously described *mnr-1* gain-of-function phenotype. When *mnr-1/menorin* is misexpressed in body wall muscles in an otherwise wild type background, PVD dendritic arbors often adopt an inappropriate shape that more closely resembles African baobab trees than the typical menorah-shaped dendrite arbors (Fig. 4E)[9]. We found that the formation of both normal and misshapen dendritic trees is completely dependent on *lect-2* (Fig. 4F). Collectively, these observations suggest that LECT-2/Chondromodulin II acts genetically downstream of MNR-1/Menorin and SAX-7/L1CAM, and upstream of the leucine rich transmembrane receptor DMA-1.

LECT-2/Chondromodulin II may be part of a complex with the SAX-7/L1CAM cell adhesion molecule

LECT-2::mNeonGreen expression was indistinguishable from a GFP reporter for SAX-7/L1CAM (Fig. 2E, F), raising the possibility that these two factors are part of a complex. We thus asked whether LECT-2/Chondromodulin II localization is dependent on factors of the menorin pathway, including SAX-7/L1CAM, MNR-1/Menorin, and DMA-1/LRR-TM. We found that LECT-2::mNeonGreen localization appeared entirely dependent on SAX-7/L1CAM, but not MNR-1/Menorin or DMA-1/LRR-TM (Fig. 4G–K). Based on these findings, we propose that LECT-2/Chondromodulin II acts as a muscle-derived cofactor of the hypodermis-expressed MNR-1/Menorin–SAX-7/L1CAM complex, which in turn interacts with the leucine rich transmembrane receptor DMA-1/LRR-TM on PVD neurons [8, 9]. LECT-2/Chondromodulin II could provide additional specificity by creating a local high affinity complex to pattern PVD dendrites, possibly through binding directly to SAX-7/L1CAM (Fig. 4L). However, LECT-2/Chondromodulin II is not an essential cofactor of SAX-7/L1CAM in general, because *lect-2* mutants do not share all phenotypes with *sax-7/L1CAM* mutants, such as maintenance defects of ventral nerve cord axons or cell body position, nor is *lect-2* required for KAL-1/Anosmin-1-dependent neurite branching like *sax-7/L1CAM* (Table S1)[27–30].

LECT-2/Chondromodulin II appears to be acting as a permissive factor much in analogy to the EGF-CFC-like secreted protein *one-eyed pinhead* in zebrafish, which regulates gastrulation by functioning as a permissive cue for nodal signaling [31, 32]. First, LECT-2/Chondromodulin II expression from essentially anywhere can rescue the mutant *lect-2* mutant phenotype, just like one-eyed pinhead rescues mutant fish cell non-autonomously [31, 32]. Second, misexpression of LECT-2 in different tissues of wild type animals, including in neurons, muscle, hypodermis, pharynx or coelomocytes failed to result in defects in PVD patterning (Fig. 3E, data not shown). However, we cannot exclude that expression from other tissues could result in a phenotype, which could thereby indicate some instructive aspects of LECT-2 function. Similarly, we cannot rule out the possibility that LECT-2 acts as a processing factor (for example as a peptidase, given its sequence similarity), which activates or inactivates one or more proteins locally as they appear on the cell surface.

How general is a developmental role for LECT-2/Chondromodulin II? It has been recently shown that neurites of hippocampal neurons show reduced length in mice lacking a functional copy of the *Lect2* locus [33, 34]. Thus, our findings suggest that (1) LECT-2/Chondromodulin II may not only function to pattern sensory neurons, but may show similar functions in the central nervous system and (2) that the developmental functions of LECT-2 may be conserved from invertebrates to vertebrates. In conclusion, our studies indicate that the concerted molecular interplay of both secreted and diffusible (e.g. LECT-2) as well as contact dependent cues (e.g. MNR-1/Menorin, SAX-7/L1CAM) from different surrounding tissues (muscle, hypodermis) orchestrate patterning of somatosensory dendrites in *C. elegans.* Given the conservation of these molecules, it will be interesting to determine whether similar mechanisms are at play in vertebrates.

Experimental Procedures

C. elegans strains and imaging

All strains were maintained using standard methods [35]. All experiments were performed at 20°C, and animals were scored as 1-day -old adults unless otherwise specified. The strains and mutant alleles used in this study are listed in the Supplemental Experimental Procedures. Fluorescent images were captured in live *C. elegans* using a Plan-Apochromat 40×/1.4 or 63×/1.4 objective on a Zeiss Axioimager Z1 Apotome. Worms were immobilized using 10 mM sodium azide and *Z* stacks were collected. Maximum intensity projections were used for further analysis.

For quantification of branching, synchronized starved L1 larvae were allowed to grow for 50 hrs (corresponding to late L4-young adulthood) at which time they were mounted and fluorescent images of immobilized animals (1–5 mM levamisol, Sigma) were captured using a Zeiss Axioimager. *Z* stacks were collected and maximum projections were used for tracing of dendrites as described [9]. Briefly, all branches within 100 μm of the primary branch anterior to the cell body were traced, measured, and classified into primary, secondary, tertiary, quaternary, and ectopic tertiary branches using the NeuronJ plugin of the ImageJ 1.46r software. Statistical comparisons were conducted using one-sided ANOVA with the

Tukey correction, the Z-test, the Kruskal-Wallis test, or the Wilcoxon rank-sum test, as applicable (Prism [GraphPad Software]).

Cloning of mutant alleles

The *rz2* allele arose spontaneously in the lab. In addition, we obtained three alleles from forward genetic screens, seven alleles from the Million Mutation Project [36] and two deletion alleles. Details on positional cloning and complementation tests are provided in Supplemental Experimental Procedures.

Molecular biology and transgenesis

To assemble tissue specific expression constructs used for rescue experiments, the *lect-2* cDNA was cloned under control of the following promoters: hypodermal *Pdpy-7* [37], body wall muscle *Pmyo-3* [38], pan-neuronal *Prab-3* [39], the coelomocyte specific *Punc-122* promoter [40], *and* an AIY-specific *Pttx-3* promoter [41]. Constructs for structure-function analyses of *lect-2* were assembled by subcloning with specific restriction enzymes or by PCR fusion based approaches. All plasmids contained the *unc-54* 3′UTR. Constructs for tissue specific rescue experiments of *lect-2* dendrite patterning were injected at 5 ng/μl together with *Pmyo-3::mCherry* or *Pceh-22::GFP* as injection markers at 50 ng/μl. For details see Supplemental Experimental Procedures.

Supplementary Material

Refer to Web version on PubMed Central for supplementary material.

Acknowledgments

We thank S. Cook, K. Gritsman, O. Hobert, R. Townley, and members of the Bülow laboratory for comments on the manuscript and for discussion during the course of this work. We thank S. Chen and S. Rodriguez for help with initial experiments; the Caenorhabditis Genome Center for strains (funded by NIH Office of Research Infrastructure Programs, P40OD010440); O. Hobert, N. Ramirez-Suarez, and K. Shen for reagents, and Yuji Kohara for the *yk2005k01* cDNA clone. This work was funded in part through the NIH (R21NS081505 to H.E.B; T32GM007288 and F31HD066967 to C.A.D.B.; T32GM07491 to M.I.L.P. and C.A.C.; P30HD071593 to Albert Einstein College of Medicine) and a Human Genome Pilot Project from Albert Einstein College of Medicine. H.E.B. is an Irma T. Hirschl/Monique Weill-Caullier research fellow.

References

1. Dong X, Shen K, Bülow HE. Intrinsic and extrinsic mechanisms of dendritic morphogenesis. Annu Rev Physiol. 2015; 77:271–300. [PubMed: 25386991]
2. Jan YN, Jan LY. Branching out: mechanisms of dendritic arborization. Nat Rev Neurosci. 2010; 11:316–328. [PubMed: 20404840]
3. Puram SV, Bonni A. Cell-intrinsic drivers of dendrite morphogenesis. Development. 2013; 140:4657–4671. [PubMed: 24255095]
4. Polleux F, Morrow T, Ghosh A. Semaphorin 3A is a chemoattractant for cortical apical dendrites [see comments]. Nature. 2000; 404:567–573. [PubMed: 10766232]
5. Meltzer S, Yadav S, Lee J, Soba P, Younger SH, Jin P, Zhang W, Parrish J, Jan LY, Jan YN. Epidermis-Derived Semaphorin Promotes Dendrite Self-Avoidance by Regulating Dendrite-Substrate Adhesion in Drosophila Sensory Neurons. Neuron. 2016; 89:741–755. [PubMed: 26853303]
6. McAllister AK, Katz LC, Lo DC. Opposing roles for endogenous BDNF and NT-3 in regulating cortical dendritic growth. Neuron. 1997; 18:767–778. [PubMed: 9182801]

7. Smith CJ, Watson JD, VanHoven MK, Colon-Ramos DA, Miller DM 3rd. Netrin (UNC-6) mediates dendritic self-avoidance. Nat Neurosci. 2012; 15:731–737. [PubMed: 22426253]
8. Dong X, Liu OW, Howell AS, Shen K. An extracellular adhesion molecule complex patterns dendritic branching and morphogenesis. Cell. 2013; 155:296–307. [PubMed: 24120131]
9. Salzberg Y, Diaz-Balzac CA, Ramirez-Suarez NJ, Attreed M, Tecle E, Desbois M, Kaprielian Z, Bülow HE. Skin-Derived Cues Control Arborization of Sensory Dendrites in Caenorhabditis elegans. Cell. 2013; 155:308–320. [PubMed: 24120132]
10. Benson MD, James S, Scott K, Liepnieks JJ, Kluve-Beckerman B. Leukocyte chemotactic factor 2: A novel renal amyloid protein. Kidney Int. 2008; 74:218–222. [PubMed: 18449172]
11. Mereuta OM, Theis JD, Vrana JA, Law ME, Grogg KL, Dasari S, Chandan VS, Wu TT, Jimenez-Zepeda VH, Fonseca R, et al. Leukocyte cell-derived chemotaxin 2 (LECT2)-associated amyloidosis is a frequent cause of hepatic amyloidosis in the United States. Blood. 2014; 123:1479–1482. [PubMed: 24415538]
12. Kameoka Y, Yamagoe S, Hatano Y, Kasama T, Suzuki K. Val58Ile polymorphism of the neutrophil chemoattractant LECT2 and rheumatoid arthritis in the Japanese population. Arthritis Rheum. 2000; 43:1419–1420. [PubMed: 10857804]
13. Lu XJ, Chen J, Yu CH, Shi YH, He YQ, Zhang RC, Huang ZA, Lv JN, Zhang S, Xu L. LECT2 protects mice against bacterial sepsis by activating macrophages via the CD209a receptor. J Exp Med. 2013; 210:5–13. [PubMed: 23254286]
14. Smith CJ, Watson JD, Spencer WC, O'Brien T, Cha B, Albeg A, Treinin M, Miller DM 3rd. Time-lapse imaging and cell-specific expression profiling reveal dynamic branching and molecular determinants of a multi-dendritic nociceptor in C. elegans. Dev Biol. 2010; 345:18–33. [PubMed: 20537990]
15. Albeg A, Smith CJ, Chatzigeorgiou M, Feitelson DG, Hall DH, Schafer WR, Miller DM 3rd, Treinin M. C. elegans multi-dendritic sensory neurons: morphology and function. Mol Cell Neurosci. 2011; 46:308–317. [PubMed: 20971193]
16. Hiraki Y, Inoue H, Kondo J, Kamizono A, Yoshitake Y, Shukunami C, Suzuki F. A novel growth-promoting factor derived from fetal bovine cartilage, chondromodulin II. Purification and amino acid sequence. J Biol Chem. 1996; 271:22657–22662. [PubMed: 8798437]
17. Yamagoe S, Yamakawa Y, Matsuo Y, Minowada J, Mizuno S, Suzuki K. Purification and primary amino acid sequence of a novel neutrophil chemotactic factor LECT2. Immunol Lett. 1996; 52:9–13. [PubMed: 8877413]
18. Rawlings ND, Waller M, Barrett AJ, Bateman A. MEROPS: the database of proteolytic enzymes, their substrates and inhibitors. Nucleic Acids Res. 2014; 42:D503–509. [PubMed: 24157837]
19. Bamford CV, Francescutti T, Cameron CE, Jenkinson HF, Dymock D. Characterization of a novel family of fibronectin-binding proteins with M23 peptidase domains from Treponema denticola. Mol Oral Microbiol. 2010; 25:369–383. [PubMed: 21040511]
20. Chen CK, Yang CY, Hua KT, Ho MC, Johansson G, Jeng YM, Chen CN, Chen MW, Lee WJ, Su JL, et al. Leukocyte cell-derived chemotaxin 2 antagonizes MET receptor activation to suppress hepatocellular carcinoma vascular invasion by protein tyrosine phosphatase 1B recruitment. Hepatology. 2014; 59:974–985. [PubMed: 24114941]
21. Bülow HE, Berry KL, Topper LH, Peles E, Hobert O. Heparan sulfate proteoglycan-dependent induction of axon branching and axon misrouting by the Kallmann syndrome gene kal-1. Proc Natl Acad Sci U S A. 2002; 99:6346–6351. [PubMed: 11983919]
22. Schroeder NE, Androwski RJ, Rashid A, Lee H, Lee J, Barr MM. Dauer-specific dendrite arborization in C. elegans is regulated by KPC-1/Furin. Curr Biol. 2013; 23:1527–1535. [PubMed: 23932402]
23. Dickinson DJ, Pani AM, Heppert JK, Higgins CD, Goldstein B. Streamlined Genome Engineering with a Self-Excising Drug Selection Cassette. Genetics. 2015; 200:1035–1049. [PubMed: 26044593]
24. Liang X, Dong X, Moerman DG, Shen K, Wang X. Sarcomeres Pattern Proprioceptive Sensory Dendritic Endings through UNC-52/Perlecan in C. elegans. Dev Cell. 2015; 33:388–400. [PubMed: 25982673]

25. Fares H, Greenwald I. SEL-5, a serine/threonine kinase that facilitates lin-12 activity in Caenorhabditis elegans. Genetics. 1999; 153:1641–1654. [PubMed: 10581273]
26. Liu OW, Shen K. The transmembrane LRR protein DMA-1 promotes dendrite branching and growth in C. elegans. Nat Neurosci. 2012; 15:57–63. [PubMed: 22138642]
27. Sasakura H, Inada H, Kuhara A, Fusaoka E, Takemoto D, Takeuchi K, Mori I. Maintenance of neuronal positions in organized ganglia by SAX-7, a Caenorhabditis elegans homologue of L1. Embo J. 2005; 24:1477–1488. [PubMed: 15775964]
28. Wang X, Kweon J, Larson S, Chen L. A role for the C. elegans L1CAM homologue lad-1/sax-7 in maintaining tissue attachment. Dev Biol. 2005; 284:273–291. [PubMed: 16023097]
29. Bénard C, Tjoe N, Boulin T, Recio J, Hobert O. The small, secreted immunoglobulin protein ZIG-3 maintains axon position in Caenorhabditis elegans. Genetics. 2009; 183:917–927. [PubMed: 19737747]
30. Diaz-Balzac CA, Lazaro-Pena MI, Ramos-Ortiz GA, Bülow HE. The Adhesion Molecule KAL-1/anosmin-1 Regulates Neurite Branching through a SAX-7/L1CAM-EGL-15/FGFR Receptor Complex. Cell Rep. 2015; 11:1377–1384. [PubMed: 26004184]
31. Gritsman K, Zhang J, Cheng S, Heckscher E, Talbot WS, Schier AF. The EGF-CFC protein one-eyed pinhead is essential for nodal signaling. Cell. 1999; 97:121–132. [PubMed: 10199408]
32. Zhang J, Talbot WS, Schier AF. Positional cloning identifies zebrafish one-eyed pinhead as a permissive EGF-related ligand required during gastrulation. Cell. 1998; 92:241–251. [PubMed: 9458048]
33. Koshimizu Y, Ohtomi M. Regulation of katanin-P60 levels by LECT2 adjusts microtubular morphology. Neuroreport. 2010; 21:646–650. [PubMed: 20463617]
34. Koshimizu Y, Ohtomi M. Regulation of neurite extension by expression of LECT2 and neurotrophins based on findings in LECT2-knockout mice. Brain Res. 2010; 1311:1–11. [PubMed: 19917270]
35. Brenner S. The genetics of Caenorhabditis elegans. Genetics. 1974; 77:71–94. [PubMed: 4366476]
36. Thompson O, Edgley M, Strasbourger P, Flibotte S, Ewing B, Adair R, Au V, Chaudhry I, Fernando L, Hutter H, et al. The million mutation project: a new approach to genetics in Caenorhabditis elegans. Genome Res. 2013; 23:1749–1762. [PubMed: 23800452]
37. Gilleard JS, Barry JD, Johnstone IL. cis regulatory requirements for hypodermal cell-specific expression of the Caenorhabditis elegans cuticle collagen gene dpy-7. Mol Cell Biol. 1997; 17:2301–2311. [PubMed: 9121480]
38. Okkema PG, Harrison SW, Plunger V, Aryana A, Fire A. Sequence requirements for myosin gene expression and regulation in Caenorhabditis elegans. Genetics. 1993; 135:385–404. [PubMed: 8244003]
39. Nonet ML, Staunton JE, Kilgard MP, Fergestad T, Hartwieg E, Horvitz HR, Jorgensen EM, Meyer BJ. Caenorhabditis elegans rab-3 mutant synapses exhibit impaired function and are partially depleted of vesicles. J Neurosci. 1997; 17:8061–8073. [PubMed: 9334382]
40. Loria PM, Hodgkin J, Hobert O. A conserved postsynaptic transmembrane protein affecting neuromuscular signaling in Caenorhabditis elegans. J Neurosci. 2004; 24:2191–2201. [PubMed: 14999070]
41. Altun-Gultekin Z, Andachi Y, Tsalik EL, Pilgrim D, Kohara Y, Hobert O. A regulatory cascade of three homeobox genes, ceh-10, ttx-3 and ceh-23, controls cell fate specification of a defined interneuron class in C. elegans. Development. 2001; 128:1951–1969. [PubMed: 11493519]
42. Papadopoulos JS, Agarwala R. COBALT: constraint-based alignment tool for multiple protein sequences. Bioinformatics. 2007; 23:1073–1079. [PubMed: 17332019]
43. Grabowska M, Jagielska E, Czapinska H, Bochtler M, Sabala I. High resolution structure of an M23 peptidase with a substrate analogue. Sci Rep. 2015; 5:14833. [PubMed: 26437833]

Highlights

- The conserved cue LECT-2/Chondromodulin II patterns somatosensory dendrite arbors
- LECT-2/Chondromodulin II acts as a muscle-derived, diffusible cue
- LECT-2 acts together with the conserved MNR-1/SAX-7/DMA-1 adhesion complex
- LECT-2/Chondromodulin II localization is dependent on skin-derived cues

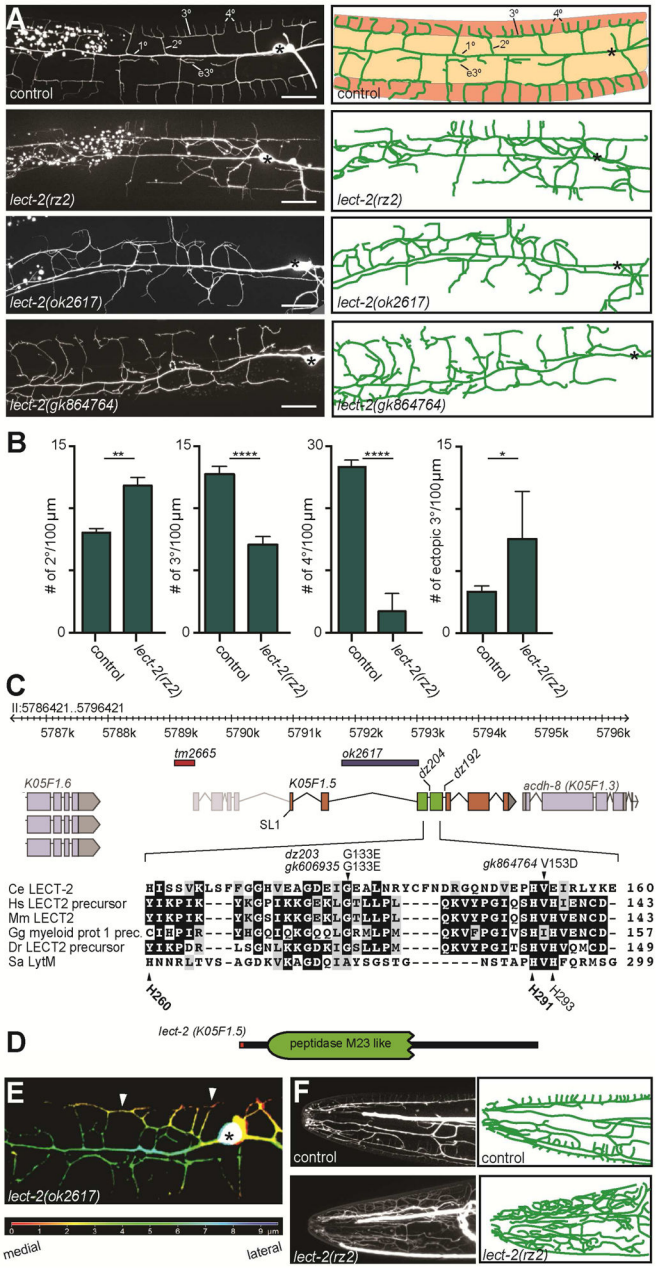

Figure 1. A LECT-2/Lect2 like chemokine is required for patterning of somatosensory dendrites

A. Fluorescent images of PVD (left panels) and schematics (right panels) of *lect-2* mutant and wild type control animals. PVD is visualized by the *wdIs52 [F49H12.4::GFP]* transgene. Primary (1°), secondary (2°), tertiary (3°), quaternary (4°), and ectopic tertiary (e3°) dendrites are indicated. Note, that tertiary dendrites follow the boundary between dorsal and ventral muscle quadrants (salmon) and lateral hypodermis (tan)(Fig. 1A)[8, 9]. Ectopic tertiary dendrites are branches that emanate from secondary branches, but not along the boundary of lateral hypodermis and muscle. Anterior is to the left and dorsal is up in all panels, scale bars indicate 20µm.

B. Quantification of secondary, tertiary, quaternary, and ectopic tertiary branch numbers. Data are represented as mean ± SEM. Statistical comparisons were performed using one-sided ANOVA with the Tukey correction. Statistical significance is indicated (*p ≤ 0.05, **p ≤ 0.01, **** ≤ 0.0001). n = 20 wild type control animals (1011 dendritic branches); n = 20 *lect-2(rz2)* mutant animals (596 dendritic branches). For data of aggregate branch length, see Fig. S3A.

C. Genomic environs of *lect-2.* A predicted longer transcript for *lect-2* (shaded), even if it exists, is not required for dendrite patterning, because the *tm2665* deletion allele displays no phenotype in PVD neurons and complements other *lect-2* alleles (see also Supplemental Experimental Procedures). The shorter *lect-2* transcript is supported by EST data (Fig. S1). Multiple sequence alignment of *C. elegans* LECT-2 (Ce; acc# KX255656), human LECT2 (Hs; acc# BAA23609.1), mouse Lect2 (Mm; acc#BAA33385.1), chick myeloid protein precursor 1 (Gg; acc# NP_990809.2), zebrafish LECT2 (Dr; acc# NP_001041520.1), and *Staphylococcus aureus NTCC8325* (Sa; acc# O33599.3) created by COBALT (constrained based multiple sequence alignment tool) [42]. Missense alleles are indicated above the alignments, and residues that are part of the putative catalytic site [43] are indicated below (bold if conserved in *C. elegans*). (see also Fig. S1, Fig. S2, and Supplemental Experimental Procedures).

D. Schematic of the *lect-2* gene, with a signal sequence indicated in red and the M23 peptidase like domain in green.

E. Maximum intensity projection of a *lect-2(ok2617)* mutant in which each optical plane is labeled in a different color (17 sections of 0.6 μm each), where warmer and colder colors indicate more medial and lateral sections of the animal, respectively. Overlapping tertiary dendrites (indicated by white arrows) appear in the same focal plane (based on the same color). Since the width of dendritic branches is approximately 200nm [15], these data suggest that tertiary dendrites are closely apposed (within 0.6 μm) or directly touching.

F. Fluorescent images of FLP (left panels) and schematics (right panels) of *lect-2* mutant and wild type control animals. FLP is visualized by the *muIs32* transgene.

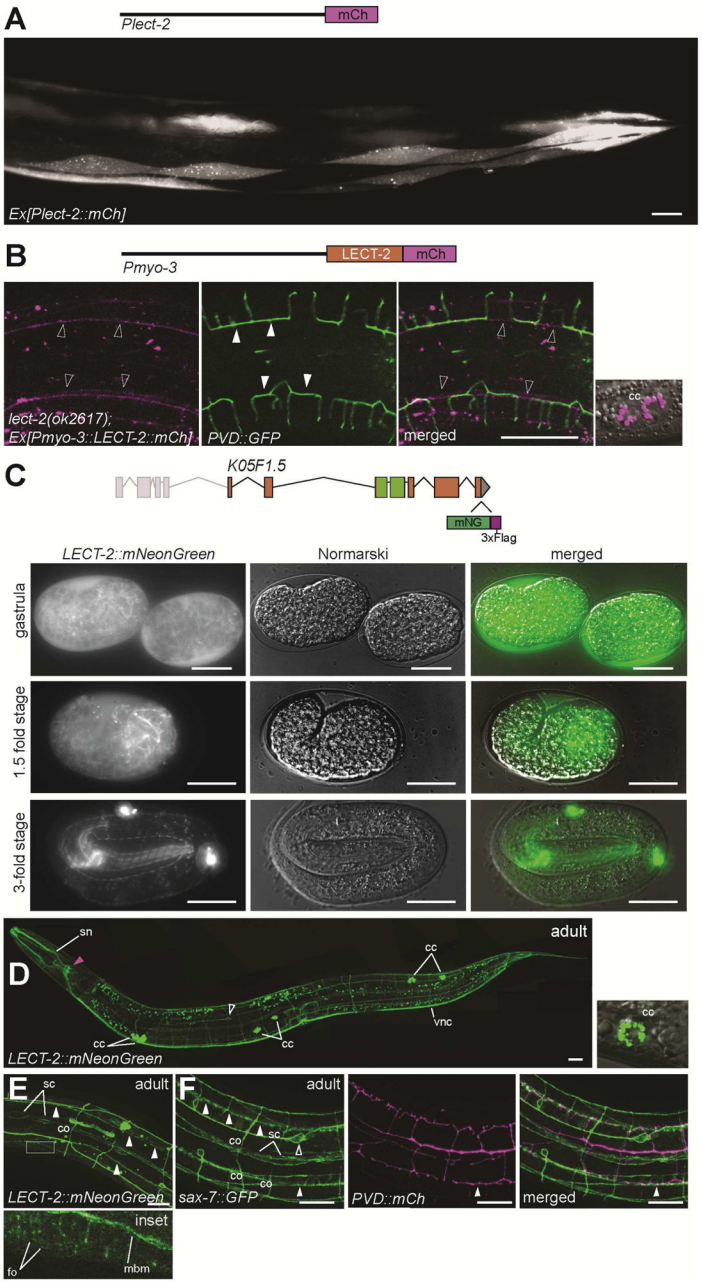

Figure 2. LECT-2/Lect2 is expressed in muscle and localizes to the nervous system and basement membranes

A. Schematic of the *lect-2* transcriptional reporter and fluorescent micrograph of an adult transgenic animal carrying the *Plect-2::mCherry* transgene. Expression is seen in body wall muscle. Anterior is to the left and dorsal up, and a scale bar indicates 20 μm in all panels.

B. Schematic of the LECT-2 translational reporter, and maximum intensity projections of an animal, showing expression of the LECT-2::mCherry translational reporter in a *lect-2* mutant background. PVD is visualized by the *wdIs52 [F49H12.4::GFP]* transgene. Vesicular coelomocyte (cc) expression is shown in a separate panel. Expression is seen along the

lateral hypodermal ridge (empty arrowheads), and continues along the tertiary line of PVD branches (white arrowheads).

C. Schematic of the CRISPR/Cas9 modified *lect-2* locus, and images of LECT-2::mNeonGreen expression at endogenous levels during different embryonic stages.

D. – E. Fluorescent micrographs of adult animals of the CRISPR/Cas9 modified LECT-2::mNeonGreen strain showing LECT-2::mNeonGreen localization at endogenous levels. Staining is seen on processes of the nervous system, including the ventral nerve cord (vnc), dendrites of sensory neurons (sn), and coelomocytes (cc, see right enlarged panel with vesicular staining). The nerve ring also shows staining (D, magenta arrowhead), but associated head neurons, located immediately posterior to the nerve ring show little or no staining. Expression is also seen surrounding the seam cells (sc), lateral hypodermal ridge (E, white arrowheads), motor neurons (see Fig. 4G) and associated commissures (co), the ventral nerve cord (vnc), the ALM mechanosensory neuron (D, empty arrowhead), as well as the basement membrane of body wall muscles (mbm) and the parallel bands of fibrous organelles (fo)(E, inset). Only weak, if any, staining was seen on PVD neurons.

F. Micrographs of the SAX-7::GFP fosmid reporter [*ddIs290*] showing expression in the same locations as LECT-2::mNeonGreen, including the seam cells (sc), lateral hypodermal ridge (white arrowhead), commissures (co), and the ALM neuron (empty arrowhead). As with the translational LECT-2 reporter shown in 2B, expression along the lateral hypodermal ridge co-localizes with the tertiary branches of PVD, visualized by the *dzIs53 [F49H12.4::mCherry]* transgene.

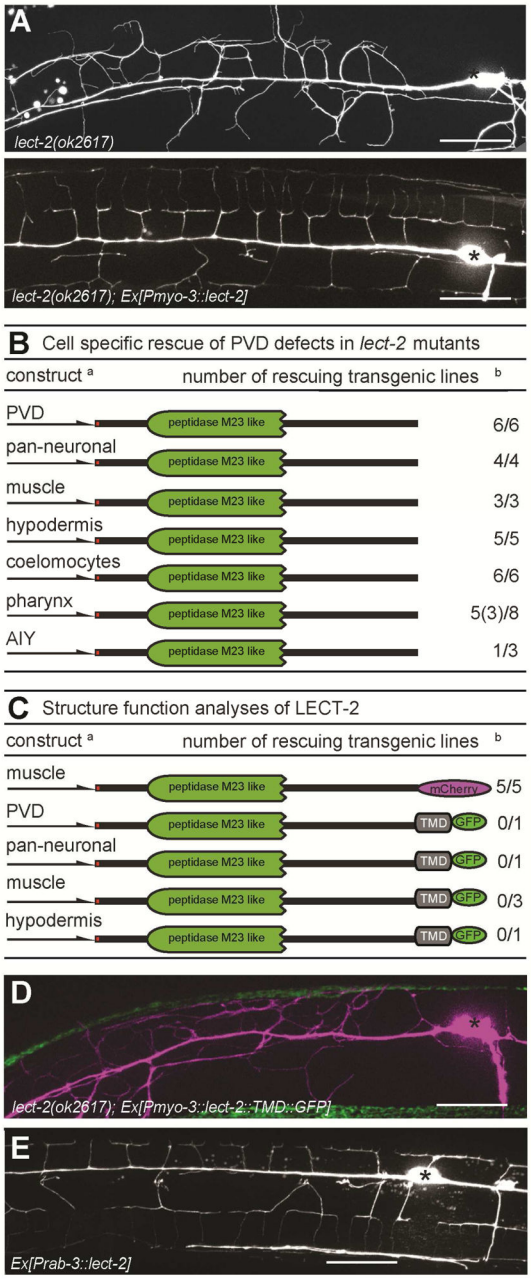

Figure 3. LECT-2/Lect2 is a muscle-derived diffusible permissive cue

A. Lateral view of a *lect-2(ok2617)* mutant animal and a transgenically rescued *lect-2(ok2617)* animal. PVD is visualized by the *wdIs52 [F49H12.4::GFP]* transgene. Anterior is to the left, dorsal up, and scale bars indicate 20 μm in all panels.

B. – C. Shown are the constructs, promoters used, and the number of rescuing lines out of the total number of lines (partial rescuing lines in parentheses). [a] Deletions are indicated as dashed lines. Color-coding and abbreviations as in Figures 2. [b] Rescue was defined as restoration of secondary, tertiary, and quaternary branches, i.e., the establishment of menorah-like structures. Partial rescue was defined as lines in which <50% of the animals

showed restoration of PVD-like branching patterns. Transgenic animals were always compared with non-transgenic siblings, except for constructs with the heterologous transmembrane domains. Number of transgenic animals scored was n = 50 per transgenic line.

D. Fluorescent image of an adult *lect-2(ok2617)* mutant animal with muscle expression of a version of *lect-2*, where the last 32 amino acids of LECT-2 were replaced with a heterologous transmembrane domain of PAT-3/β-integrin, followed by GFP (*Pmyo-3::lect-2::TMD::GFP*, upper panel, PVD visualized by the *Pser2prom3::mCherry* co-injection marker).

E. Fluorescent image of an adult wild type animal expressing LECT-2 pan-neuronally (*Prab-3::LECT-2*, lower panel, PVD is visualized by the *wdIs52 [F49H12.4::GFP]* transgene).

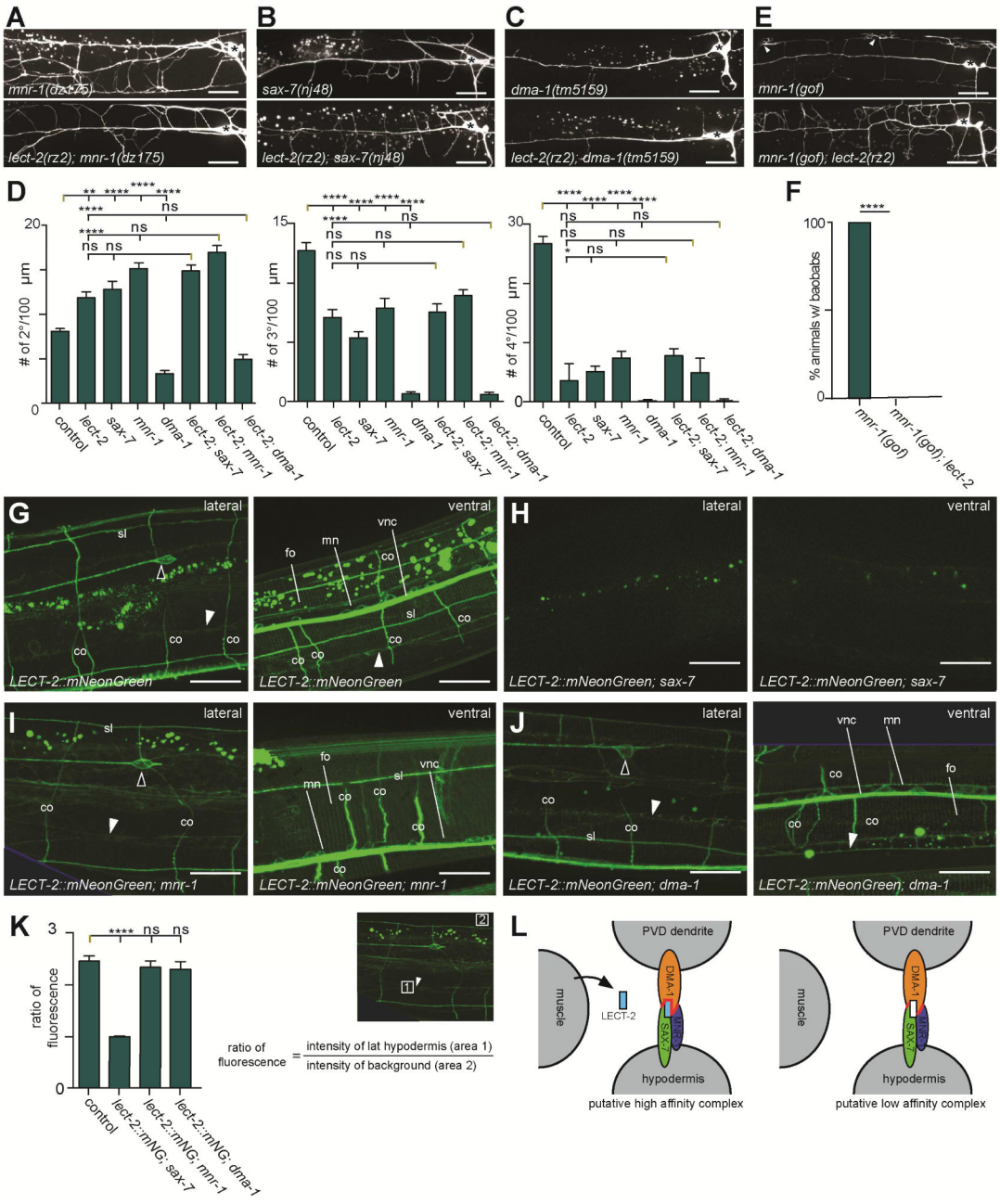

Figure 4. LECT-2/Lect2 acts downstream of menorin within the menorin pathway

A. – C. Fluorescent images of animals of the indicated genotypes. Anterior is to the left, dorsal up, and scale bars indicate 20 µm in all panels.

D. Quantification of branch number in *lect-2(rz2)*, *sax-7(nj48)*, *mnr-1(dz175)*, *dma-1(tm5159)* single- and double-mutant animals. Data are represented as mean ± SEM. Statistical comparisons were performed using one-sided ANOVA with the Tukey correction and statistical significance is indicated (*p ≤ 0.05, **p ≤ 0.01, ***p ≤ 0.001 ****p ≤ 0.0001; ns: not significant [p > 0.05]). n = 20 wild type controls (1011 dendritic branches); n = 20 *lect-2(rz2)* mutant animals (596 dendritic branches); n = 20 *mnr-1(dz175)* mutant animals

(831 dendritic branches); n = 20 *sax-7(nj48)* mutant animals (633 dendritic branches), n = 20 *dma-1(tm5159)* mutant animals (86 dendritic branches), n = 20 *lect-2(rz2); sax-7(nj48)* mutant animals (814 dendritic branches), n = 20 *lect-2(rz2); mnr-1(dz175)* mutant animals (849 dendritic branches), n = 20 *dma-1(tm5159); lect-2(rz2)* mutant animals (135 dendritic branches). Data for wild type control and *lect-2* animals in (D) are identical to those in Figure 1 and are shown for comparison only. For data of aggregate branch length, see Fig. S3C.

E. Fluorescent images of the *mnr-1(gof)* strain (*dzIs43*) in the genotypes indicated. Baobabs are indicated by white arrowheads.

F. Quantification of animals containing baobabs in *mnr-1(gof)* and *mnr-1(gof); lect-2(rz2)* animals. N=100 for each genotype. Data are represented as mean ± standard error of proportion. Statistical comparisons were performed using the Z-test and statistical significance is indicated: ****$p \leq 0.0001$.

G. – J. Fluorescent images of adult animals (left panel, lateral view and right panel ventral view) of the genotypes indicated. Ventral nerve cord (vnc), fibrous organelles (fo), commissures (co), motor neurons (mn), lateral hypodermal ridge (white arrowheads), and the ALM neuron (empty arrowhead). Vesicular staining in coelomocytes was unaffected in different genetic backgrounds (data not shown).

K. Quantification of fluorescence. The ratio of fluorescence was calculated as the quotient of the average fluorescence in area 1 (at the boundary of muscle and hypodermis) and background (area 2). N=15 for each genotype. Statistical significance was calculated using the Kruskal-Wallis test. Data are represented as mean ± SEM, and statistical significance is indicated as ****$p \leq 0.0001$; ns, not significant [$p > 0.05$].

L. Putative model of a high affinity or low affinity complex. A hypothetical molecular interaction surface (indicated in red) is enlarged by LECT-2/Chondromodulin II in the high affinity complex.